

Award Accounts

The Chemical Society of Japan Award for Technical Development for 2003

Development of Innovative Three-Way Catalysts Containing Ceria–Zirconia Solid Solutions with High Oxygen Storage/Release Capacity

Masahiro Sugiura,* Masakuni Ozawa,[1] Akihiko Suda, Tadashi Suzuki, and Takaaki Kanazawa[2]

Applied Catalysis Lab., Toyota Central R&D Labs. Inc., Nagakute, Aichi 480-1192

[1]Ceramics Research Lab., Nagoya Institute of Technology, Tajimi, Gifu 507-0017

[2]Catalyst Design Dept., Material Engineering Div. I, Toyota Motor Corp., Toyota-cho, Toyota, Aichi 471-8572

Received July 28, 2004; E-mail: sugiuram@spring8.or.jp

Innovative three-way catalysts containing ceria–zirconia solid solutions (CZ) with a ZrO_2 content ranging from 5 to 75 mol% were developed. Such catalysts have very high oxygen storage/release capacity (OSC). The OSC of catalysts containing first-generation CZ was found to increase linearly with the amount of zirconia dissolved in the solid solution in the 0–20 mol% ZrO_2 range. The thermal stability of the catalyst containing first-generation CZ was higher than that containing ceria. Second-generation CZ with greater OSC than first-generation CZ was developed by a homogeneous coprecipitation process, followed by heat-treatment below 1000 °C, enabling dissolution of zirconia into ceria up to 75 mol% zirconia as estimated by XRD. Third-generation CZ, CZ-doped alumina (ACZ), was developed by homogeneous coprecipitation based on the "diffusion barrier concept". The OSC of ACZ was 23 times larger than that of pure ceria. The NOx emission over the catalyst containing ACZ was reduced by about a factor of five compared with that containing pure ceria. Toyota Motor Corp. has put three-way catalysts containing first-, second-, and third-generation CZ into practical use globally.

Two fundamental technologies are used consistently in automotive catalysis for purifying pollutants in the exhaust from internal combustion engines; one concerned with control of precious metals, the other with exchange of oxygen. In the former technology, precious metal particles are always controlled in a state of high dispersion, in which their catalytic activity is maintained high on the catalysts. In the latter technology, oxygen is exchanged between the catalyst and the exhaust gas. The diluted pollutants in the exhaust gas need to be enriched on the precious metal catalysts (e.g., Pt, Rh, Pd),[1,2] and simultaneously, the activity of the catalysts maintained at a maximum. The conversion rate of pollutants needs to approach 100% at the stoichiometric point[3,4] so that the exhaust contains neither excess nor insufficient oxygen. Thus, for the catalyst to store oxygen under oxygen-rich conditions and release oxygen under oxygen-lean conditions, it is essential that constituents of the exhaust gases be maintained at the stoichiometric point of the catalyst. The two technologies mentioned above constitute the foundation of research and development on automotive catalysts, even if they face stricter exhaust emission regulations. This review is mainly concerned with the exchange of oxygen.

The automotive three-way catalyst system operates under a certain range of air-to-fuel (A/F) ratios, controlled by an electric fuel-injection system[5–9] linked to an oxygen sensor device.[10–12] However, even the exhaust gases controlled by the system alternate between slightly rich to slightly lean conditions with an inevitable time lag in the system as it adjusts the ratio. This time lag lowers the conversion rate of the pollutants on precious metal catalysts, especially when the difference between their degrees of enrichment on the catalyst is large and the alternating period is long. This problem is largely solved by the use of an oxygen storage material[13–15] as a catalyst component. The material stores oxygen during oxygen-lean conditions and releases it during oxygen-rich conditions.

Since transition metals such as copper, iron, cobalt, and nickel have the capability to change their valence state, all of their oxides could store and release oxygen in exhaust gas containing a large amount of carbon dioxide. In 1972, researchers found that copper/copper oxide can both store and release oxygen in an automotive exhaust system.[16–19] However, materials such as copper/copper oxide can easily fragment, which is accompanied by a large volume change. Thus, copper/copper oxide could not be used in practice in our Toyota vehicles. This problem was finally solved (for the most part) by the use of an oxygen storage medium such as a ceria (CeO_2)[15,20–23] or ceria–lanthana (CeO_2–La_2O_3) solid solution[24–27] as a catalyst component because ceria retains its cubic

Published on the web May 6, 2005; DOI 10.1246/bcsj.78.752

crystal structure even during the alternate storage and release of oxygen and its volume change is very small. However, a small amount of iron(III)/iron(II) oxide has been used as a component of automotive catalysts.[28,29] In 1980, the use of NiO with CeO_2 in three-way catalyst systems was explored by Cooper and Keck with respect to transient oxygen storage and water gas shift activity observed in lean-rich-lean exhaust composition experiments.[30,31] Thus, oxygen storage/release on transition metals/metal oxides in exhaust gases has been a fundamental concept in automotive catalysts for the past 30 years or more.

In 1977, the Toyota Motor Corp. in Japan utilized a three-way catalyst in the exhaust system of an automobile powered by a spark ignition combustion engine for the first time.[32] The catalyst was aimed at the simultaneous purification of pollutants such as carbon monoxide (CO), hydrocarbons (HCs), and nitrogen oxides (NOx).

Common three-way catalysts mainly consist of precious metals (platinum (Pt), rhodium (Rh), and/or palladium (Pd)) on an alumina support with an oxygen storage material, usually ceria (CeO_2), as an auxiliary catalyst. The addition of CeO_2 into the three-way catalyst improves the dynamic performance for the simultaneous removal of CO, HCs, and NOx. In an exhaust gas with rich-lean A/F variation, CeO_2 in the catalyst can provide oxygen for oxidizing CO and HCs adsorbed on the catalyst under oxygen-lean conditions to CO_2 and H_2O, and can remove oxygen on the catalyst for reducing NOx adsorbed on the catalyst to nitrogen (N_2) under oxygen-rich conditions. Ce^{4+} changes spontaneously into Ce^{3+} in the CeO_2 lattice under oxygen-lean conditions and Ce^{3+} changes spontaneously into Ce^{4+} in the CeO_2 lattice under oxygen-rich conditions, owing to its non-stoichiometric behavior.[21] However, oxygen is only used on the surface of CeO_2. Besides, use of the catalyst in the automotive engine system under severe thermal conditions leads to significant degradation including loss of the specific surface area of alumina, sintering of precious metals supported on alumina and deactivation of cerium contained in the catalyst. Such problems have been largely solved by development of the oxide solid solution in the CeO_2–ZrO_2 system and the application of the solid solution to the three-way catalyst.[33–36]

1. Three-Way Catalyst Containing First-Generation CZ

In 1985, we conducted an important study on zirconia supports for automotive Pt/Rh catalysts and oxygen sensors. Yttrium-stabilized zirconia (YSZ) has been employed as a solid-state electrode for oxygen sensors.[6,10,37,38] YSZ has a higher ionic conductivity[39] due to the ease of migration of oxygen ions above 300 °C because of oxygen defects present in YSZ. However, the valences of zirconium(IV) and yttrium(III) ions in YSZ hardly change with oxygen pressure in simulated exhaust gases, according to our unpublished data. This implies that the level of oxygen defects is constant in pure oxides such as ZrO_2 and Y_2O_3. We assumed that the oxygen mobility in zirconia is high if zirconia is stabilized by cerium ions. Moreover, due to the possible valence change of the cerium ion from III to IV or from IV to III, cerium-stabilized zirconia or zirconia-stabilized ceria should have the ability to store or release more oxygen, thus, the valence change should be accompanied by an increase/decrease in the number of oxygen defects.

Table 1. Phases Formed in the CeO_2–ZrO_2 ($Ce_{1-x}Zr_xO_2$) System at 1000 °C[40]

X	Phase	Lattice constant /nm	Crystallite size /nm	Surface area /$m^2\ g^{-1}$
0	CeO_2	0.5412	110	2.9
0.1	CeO_2s.s.	0.5391	22	9.1
0.15	CeO_2s.s.	0.5385	16	—
0.2	CeO_2s.s.	0.5380	12	9.5
0.25	CeO_2s.s.	0.5381	11	—
0.3	CeO_2s.s. + C_1	0.5381	9	12.5
0.4	CeO_2s.s. + C_1	—	—	—

s.s.: solid solution; C_1: zirconium-rich complex oxide.

Based on this principle, a new oxygen storage material, namely first-generation CZ, and three-way catalysts containing this material were developed in 1987 and in 1989, respectively.[33,34] The three-way activity of these catalysts was enhanced through the combined use of CZ and lanthana or ceria–zirconia–lanthana solid solutions or solutions comprising ceria, zirconia and another rare earth metal oxide such as Y or Nd oxide. This chapter focuses on the effect of OSC and describes the activity of three-way catalysts containing first-generation CZ on the lattice constant, relative surface area, and particle size of CZ.

Table 1 shows the crystal phase, lattice constant, crystallite size and surface area of ceria–zirconia mixed oxides ($Ce_{1-x}Zr_xO_2$) for different zirconia contents ($0 \leq x \leq 0.3$) prepared by impregnation using CeO_2 powder and aqueous zirconium(IV) bis(nitrate) oxide hydrate, followed by heat-treatment at 1000 °C.[40] As shown in the table, in the range of $0 \leq x \leq 0.2$, the lattice constant decreases linearly with the amount of zirconia dissolved in the ceria–zirconia mixed oxide ($Ce_{1-x}Zr_xO_2$). CZ in the $0.05 \leq x \leq 0.2$ range is called first-generation CZ. This is explained by the different in the radii of Ce^{4+} (0.10 nm) and Zr^{4+} (0.084 nm) ions in an oxide solid solution with a fluorite-type structure.[41] The results indicate the formation of a cubic phase solid solution of $Ce_{1-x}Zr_xO_2$ ($x \leq 0.2$), which is consistent with the phase diagram in previous studies.[42–44] The data also suggest that the dissolution of zirconia into ceria prevents the grain growth of ceria crystallites at high temperatures and thus improves the thermal stability of ceria. OSC involves the catalytic reaction of a reactant such as CO with oxygen at a surface active site of ceria. Figure 1 shows the oxidation activity of CO to CO_2 on $Ce_{1-x}Zr_xO_2$ ($x = 0$, 0.1, 0.2, 0.3) at varying temperatures (up to 600 °C) and CO pulse numbers at 600 °C.[40,45] As shown in Fig. 1, the dissolution of zirconia into ceria substantially improves the oxidation activity of CO. Figure 2 shows the average conversion of CO and NO over model alumina-supported platinum catalysts containing $Ce_{1-x}Zr_xO_2$, CeO_2, ZrO_2 without any oxygen storage material under static and dynamic conditions at 550 °C.[40,45] The gases used were (a) a constant composition stream with an A/F ratio of 14.6 (static condition) and (b) a cycled feed stream with an A/F ratio amplitude of 4% at 1 Hz with a time average A/F ratio of 14.6 (dynamic condi-

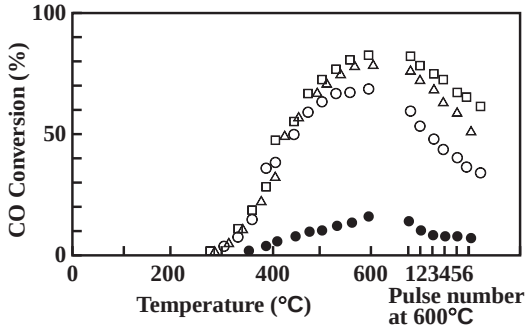

Fig. 1. Oxidation of CO pulse reaction on $Ce_{1-x}Zr_xO_2$: ●, $x = 0$; ○, $x = 0.1$: □, $x = 0.2$; ▲, $x = 0.3$.[40,45]

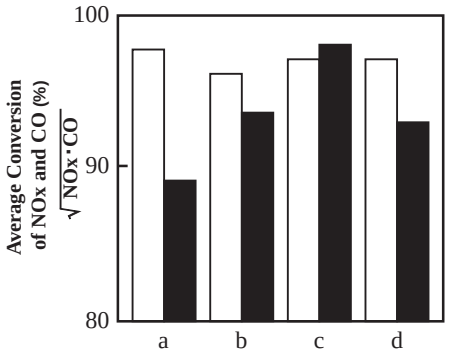

Fig. 2. Average conversion of CO and NO under static (□) and dynamic (■) conditions at 550 °C for model platinum (0.5 wt %) catalysts with and without ceria–zirconia mixed oxides: columns a, Pt/Al_2O_3; columns b, $Pt/Al_2O_3 + CeO_2/Al_2O_3$; columns c, $Pt/Al_2O_3 + Ce_{1-x}Zr_xO_2/Al_2O_3$; columns d, $Pt/Al_2O_3 + CeO_2/Al_2O_3 + ZrO_2/Al_2O_3$.[40,45]

tion). The conversion data in Fig. 2 show that the static performance is almost exactly the same over the catalysts with and without $Ce_{1-x}Zr_xO_2$ solid solution, however, the dynamic performance of the catalysts without $Ce_{1-x}Zr_xO_2$ solid solution is lower than the static performance of the same catalysts because of the deviation from the stoichiometric A/F ratio in the dynamic measurement. That is to say, the conversion data obtained under dynamic conditions revealed that the activity for CO and NO removal was more enhanced by the addition of $Ce_{1-x}Zr_xO_2$ solid solution than by that of only CeO_2. This indicated that the ceria–zirconia solid solution was a promising oxygen storage material in a three-way catalyst. Thus, a high performance three-way catalyst was designed on the basis of the research on complex oxides in the ceria–zirconia system. Catalysts containing $Ce_{1-x}Zr_xO_2$ solid solutions were subjected to tests under several modes of engine operation to evaluate their performance. Figure 3 shows the activities of the developed catalyst containing $Ce_{1-x}Zr_xO_2$ solid solution and the reference catalyst containing ceria under severely high temperature, simulating use in the USA and Europe.[46] The application of the ceria–zirconia solid solution in practical catalysts resulted in a significant improvement in catalytic removal performance of CO, NOx, and HCs as well as long-term durability under the high thermal stress which occurs for engines in the

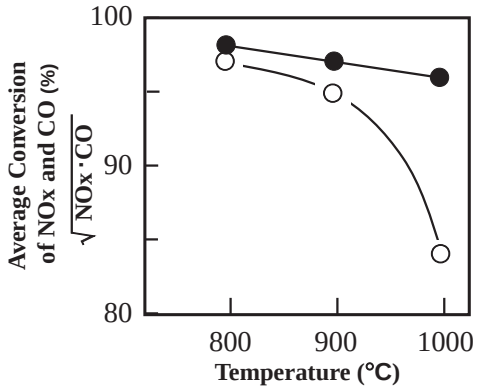

Fig. 3. Average conversion of NOx and CO as a function of temperature in durability tests at temperatures simulating use in Europe: ●, $Pt/Rh/Ce_{1-x}Zr_xO_2/Al_2O_3$; ○, $Pt/Rh/CeO_2/Al_2O_3$.[46]

USA and Europe.[45,46] Thus, in 1989, three-way catalysts containing first-generation CZ were installed in vehicles to meet the exhaust regulations in Europe and other countries.

Many studies have been conducted on ceria–zirconia solid solutions for automotive exhaust catalysts since the subject was first reported in the patent literature[33,34] and papers[40,45] by Ozawa et al. Studies on the use of ceria-based oxides in automotive three-way catalysts were summarized and presented in great detail by Kašpar et al.[47] Many research groups reported the OSC of ceria–zirconia mixed oxides fabricated by high energy mechanical milling in dry conditions,[48,49] impregnation,[35,40] conventional and modified coprecipitation,[50–55] and sol–gel processes[55–63] followed by heat-treatment below 1000 °C in air, and the same processes under reduced pressure.

2. Three-Way Catalyst Containing Second-Generation CZ

How can we develop a new process to prepare a nearly perfectly homogeneous solid solution of ceria–zirconia? This was one of the most important themes for improvement in three-way catalysts in the early 1990s. In addition, the prepared ceria–zirconia solid solution should be of a single phase, preferably a cubic phase, rather than a double or mixed phase. The assumption was that a single phase solid solution would not experience a large volume change and fragment, and would be retained in the same phase under cycling of oxygen-rich and oxygen-lean conditions at high temperature. We also assumed that it would be easier to store oxygen in, and release oxygen from, the lattice of a cubic phase oxide than from that of a tetragonal or monoclinic phase oxide.

The thermodynamically stable cubic phase of the ceria–zirconia solid solution has already been identified in the ZrO_2–CeO_2 system.[42–44,64–66] The phase diagrams reveal that zirconia is almost 100% soluble in ceria when a 50/50 mixture of Ce/Zr is heated to approximately 1600 °C in air. These solid solutions exhibit a high OSC.[67] However, their specific surface area is too low to allow their use as automotive catalysts because, as mentioned earlier, a low specific surface area restricts the rate of oxygen storage/release.

For use as an oxygen storage component of an automotive catalyst, a ceria–zirconia solid solution needs to be prepared with large specific surface area and a zirconia content of not

less than 20 mol%, and if possible, above 50 mol% to enhance OSC.

2.1 Preparation Process and Structure of Second-Generation CZ. Among the processes we investigated for preparing ceria–zirconia solid solutions by heat-treatment below 1000 °C in air, we will elaborate on a modified coprecipitation process using surfactant and/or oxidizer followed by heat-treatment (called "homogeneous coprecipitation"),[68] and on near-room-temperature synthesis of ceria–zirconia solid solutions by milling ceria powder using a zirconia mill and zirconia balls in ethanol or water (called "high-energy wet attrition milling").[69–71]

Certain solid solutions can easily be fabricated using the coprecipitation process with aqueous solutions as starting materials. The conventional coprecipitation process typically involves two steps: (i) obtaining a precipitate such as a hydroxide by adding an alkali such as ammonia to an aqueous solution of several elements to neutralize, precipitate, and age; and (ii) obtaining an oxide solid solution by heating the precipitate. In the conventional coprecipitation process, however, as the pH value of the neutral point at which ions are neutralized and precipitate upon the addition of an alkali is different for cerium and zirconium ions, the composition of a coprecipitate from cerium and zirconium ions is not always uniform.[50] The neutral point of Ce^{4+}, Zr^{4+}, and Ce^{3+} with alkalis in aqueous solution strongly depends on the pH value of the aqueous solution: Ce^{4+} reacts spontaneously with alkalis at a pH of about 1.0, Zr^{4+} in the pH range of 2.4–16, and Ce^{3+} in the pH range of 7.3–7.6.[72] Thus, a perfect solution is unlikely to be obtained by the conventional coprecipitation process. Further dissolution will occur by heat-treatment at 500 to 900 °C to produce a powder, however, the powder will not always be perfectly homogeneous due to the different pH values for coprecipitation of cerium and zirconium ions. Depending on the heat-treatment, grain growth and sintering will easily form multiple phases, such as cubic and tetragonal, as the cubic phase is compatible with CeO_2 (e.g., $CeO_2(ZrO_2)$ solid solution) and the tetragonal phase is compatible with ZrO_2 (e.g., $ZrO_2(CeO_2)$ solid solution) at temperatures below 1000 °C.[50] Thus, the specific surface area of the powder is decreased, and the particle diameter of the crystallites in the powder is increased.

The concept of the process for forming a perfectly homogeneous solution of ceria and zirconia by conventional homogeneous coprecipitation is shown in Fig. 4. As shown in the figure, the new concept entails forming precipitate nuclei of Ce–O–Zr on the hydrophilic side of a micelle formed from a surfactant such as alkylbenzenesulfonic acid.[68] The nuclei are obtained by adding the surfactant and an alkali such as ammonia to an aqueous solution containing cerium and zirconium ions. Preparation in these conditions leads to interaction between the hydrophilic group of the surfactant and the nucleus of the precipitated hydroxide. Subsequent heat-treatment yields uniformly condensed solid solution particles. Thus, the surfactant improves the homogeneity of the precipitate particles. As a result, the solid solubility is promoted, and the average diameter of crystallites is reduced. Thus, a ceria–zirconia solid solution with a high solid solubility of zirconia in ceria can be prepared using the homogeneous coprecipitation process followed by

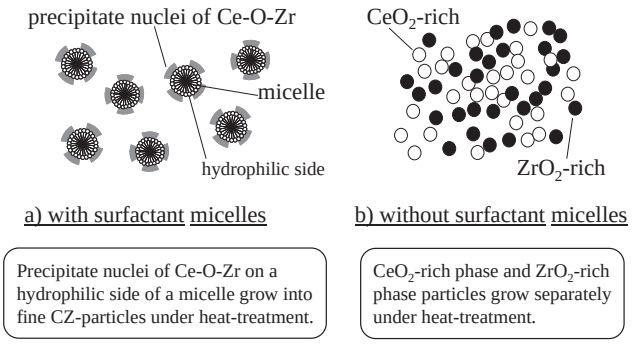

Fig. 4. Schematic mechanism of promotion of perfect dissolution in each oxide of plural oxides by homogeneous coprecipitation. a) with surfactant micelles: precipitate nuclei of Ce–O–Zr on the hydrophilic side of a micelle grow into fine CZ-particles under heat-treatment. b) without surfactant micelles: CeO_2- and ZrO_2-rich phase particles grow separately under heat-treatment.

heat-treatment below 1000 °C. The solid solubility of zirconia in ceria–zirconia mixed oxides should be defined by the following equation:

$$\begin{aligned}&\text{the solid solubility of zirconia}\\&\text{in a ceria–zirconia mixed oxide (\%)}\\&= 100 \times (\text{the amount of zirconia dissolved}\\&\text{in the total amount of ceria})\\&/(\text{the total amount of zirconia}).\end{aligned} \quad (1)$$

The solid solubility, s, of the ceria–zirconia mixed oxides can be expressed by:

$$s = (x/C)(100 - C)/(100 - x) \times 100, \quad (2)$$

where x is given by equation (3) and C is the zirconia content (mol%) of the ceria–zirconia mixed oxides.

$$x = (5.423 - a)/0.003, \quad (3)$$

where a is the lattice constant (Å) of the ceria–zirconia mixed oxide for a given zirconia content, and x is the amount of zirconia (mol%) dissolved in the ceria–zirconia solid solution. When x is 0% or 100%, the lattice constant attains the values indicated on the JCPDS (Joint Committee on Powder Diffraction Standards) card as the lattice constants for pure ceria and cubic zirconia, i.e., 0.54 and 0.51 nm, respectively.[73] Based on equations (1) to (3), the solid solubility of ceria–zirconia mixed oxides is drawn as a series of solid lines in Fig. 5, which plots a as a function of C.

Figure 5 plots the lattice constant calculated from the (311) phase of the fluorite type structure found in the ceria–zirconia mixed oxides as a function of zirconia content for oxides prepared by homogeneous coprecipitation using an aqueous solution containing cerium(III) nitrate, zirconium(IV) bis(nitrate) oxide hydrate, hydrogen peroxide, and alkylbenzenesulfonic acid mixed in the molar ratios Ce/Zr = 75/25, 7/3, 6/4, 5/5, 4/6, 3/7, and 25/75, followed by heating in air at 400 °C.[68] The lattice constant of the mixed oxides follows Vegard's rule,[74] where the lattice constants of pure ceria and cubic zirconia are 0.54 and 0.51 nm,[73] respectively. This indicates that ceria and zirconia form an almost perfectly homoge-

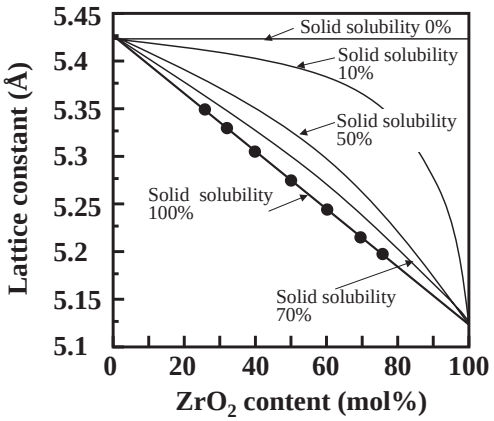

Fig. 5. The solid solubility of zirconia in ceria and the lattice constant of the fluorite-type structure as a function of zirconia content in a ceria–zirconia mixed oxide.[68]

neous solution in mixed oxides containing less than 75 mol% zirconia. The solid solubility of zirconia in these mixed oxides was 100%. XRD results indicated that the mixed oxides had a uniform, cubic fluorite-type structure, although the structure has to be identified from Raman spectra of the solid solutions in the strict crystallographic sense.[56,66] No other phase, such as ZrO_2, was detected, at zirconia contents of 0 to 75 mol%, and surprisingly, the solid solubility of zirconia in the ceria–zirconia mixed oxides was almost 100% above 50 mol% ZrO_2. In the absence of a surfactant, the solid solubility of zirconia in the mixed oxide (Ce/Zr = 50/50) was 38%; in the absence of surfactant and hydrogen peroxide, that value was 18%. The reason why the solid solubility is lower in the absence of hydrogen peroxide is because fewer cerium(III) ions replace cerium(IV) ions without an oxidizing agent in the aqueous solution. However, even if cerium(IV) nitrate is used with zirconium(IV) bis(nitrate) oxide hydrate as a starting material, the solid solubility is increased by the ultra-high-speed agitation in the aqueous solution or by the addition of a large amount of surfactant in the coprecipitation process.[68]

Figures 6 and 7 show, respectively, the X-ray diffraction patterns of ceria–zirconia mixed oxides ($Ce_{1-x}Zr_xO_2$) prepared by high-energy attrition milling (S-CZ) formed during the milling of CeO_2 powder (120 m^2/g, corresponding to 7 nm) with a zirconia mill and zirconia balls in ethanol near room temperature[69–71] and those prepared by reduction at 1200 °C in the presence of graphite (R-CZ) followed by heating at 500 °C in air.[75] The crystal structures of these oxides are summarized in Table 2.[76] All S-CZs have a uniform, cubic fluorite-type structure with a crystallite size approaching 20 nm, as estimated from the specific surface area of approximately 45 m^2/g with increasing milling time.[71] Trovarelli et al.[49] have also reported a cubic fluorite-structured CeO_2–ZrO_2 prepared by a 9-h high-energy mechanical milling run using CeO_2 and ZrO_2 as starting materials under dry conditions, similar to S-CZ55. On the other hand, the reduced mixed oxide (R-CZ) exhibits various crystal phases depending on zirconia content. R-CZ at $0.3 \leq x < 0.5$ is found to be a κ-$CeZrO_4$ phase-ceria solid solution, while R-CZ at $0.5 < x \leq 0.8$ is found to be a mixture of the κ-$CeZrO_4$ phase and tetragonal ZrO_2.

Figure 8 shows the Ce/Zr atomic ratio in nanometer-sized

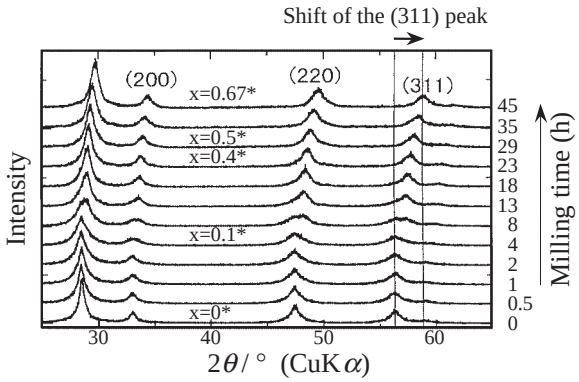

Fig. 6. X-ray diffraction patterns of ceria–zirconia mixed oxides (S-CZ) prepared by high-energy attrition milling in ethanol: x is in the formula of $Ce_{1-x}Zr_xO_2$.[69–71]

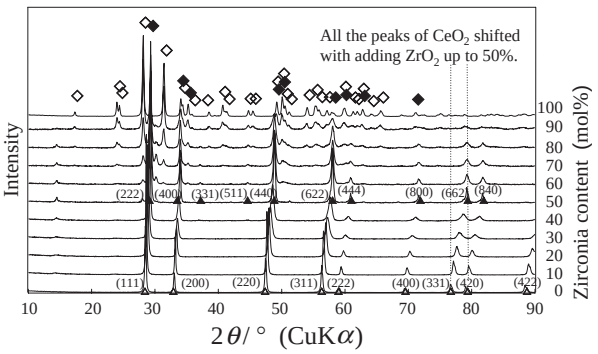

Fig. 7. X-ray diffraction patterns of ceria–zirconia mixed oxides (R-CZ) prepared by reducing at 1200 °C in the presence of graphite, followed by heating at 500 °C in air: △: fluorite structure of ceria; ▲: κ-$CeZrO_4$ phase; ◇: monoclinic zirconia; ◆: tetragonal zirconia.[75]

regions in TEM images of Pt/CeO_2–ZrO_2 determined by EDX (energy dispersion X-ray spectroscopy) analysis during TEM observations.[77] Although the Ce/Zr ratio for R-CZ at $x = 0.5$ (R-CZ55) is almost constant at 1.0, this ratio varies between 0.2 and 1.4 for S-CZ at $x = 0.5$ (S-CZ55). This means that the distribution of zirconium ions in the CeO_2 framework in S-CZ55 is not as homogeneous as in R-CZ55.[77] This is confirmed by X-ray absorption fine structure analysis.[78,79] On the basis of these analyses, Figure 9 schematizes the atomic coordination in S-CZ55, R-CZ55, and cubic ceria and zirconia, viewed normal to the (100) plane.[78–80] R-CZ55 has almost the same structure as κ-phase $CeZrO_4$, in which the atomic coordination is in an ordered state, as described by Kishimoto et al.[81,82] S-CZ55 is assumed to have the same structure as the solid solution with an irregular distribution of cerium and zirconium ions. A mixed oxide (Ce/Zr = 50/50) prepared by the above homogeneous coprecipitation process would have the same structure as that of the solid solution with an irregular distribution of cerium and zirconium ions similar to S-CZ55.

Figures 10 and 11 show the lattice constants calculated using the (311) peak of the fluorite structure in S-CZ and R-CZ, respectively, as a function of the amount of zirconia.[69,75,83] In Fig. 11, the (622) peak ascribable to the pyroclore structure (κ-phase $Ce_2Zr_2O_8$) was regarded as the (311) peak of fluorite

Table 2. Structure of Ceria–Zirconia Mixed Oxides, $Ce_{1-x}Zr_xO_2$[76]

Symbol	x	Crystal phase	Material[a)]
S-CZ	$x = 0$	cubic	ceria
S-CZ	$0 < x \leqq 0.7$[b)]	cubic	ceria–zirconia s.s
(S-CZ55	$x = 0.5$	cubic	ceria–zirconia s.s)
R-CZ	$x = 0$	cubic	ceria
R-CZ	$0 < x < 0.3$	cubic	ceria–zirconia s.s
R-CZ	$0.3 \leqq x < 0.5$	cubic	κ-$CeZrO_4$ phase-ceria s.s
R-CZ55	$x = 0.5$	cubic	κ-$CeZrO_4$ phase
R-CZ	$0.5 < x \leqq 0.8$	cubic, tetragonal	κ-$CeZrO_4$ phase-zirconia mix
R-CZ	$x = 0.9$	tetragonal, monoclinic	zirconia-κ-$CeZrO_4$ phase mix
R-CZ	$x = 1$	tetragonal, monoclinic	zirconia

a) s.s: solid solution, mix: mixture. b) S-CZ is a s.s. even in the range of $0.7 \leqq x$, when it takes time longer than 45 h to mill according to our unpublished data and the ceria–zirconia mixed oxides prepared by the homogeneous coprecipitation process with aqueous ammonia using Ce(III) nitrate and Zr(IV) bis(nitrate) oxide hydrate, are also s.s. similar to S-CZ, as estimated XRD results.[68]

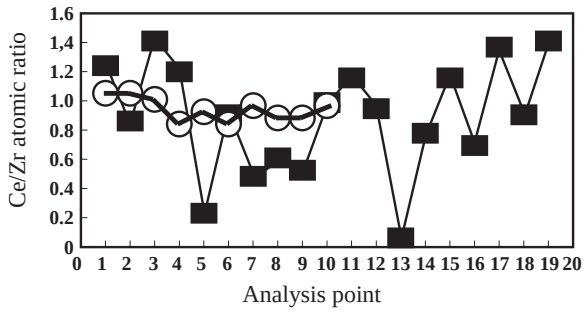

Fig. 8. Ce/Zr atomic ratio in Pt/CeO_2–ZrO_2 determined by EDX: ○: Pt/R-CZ55 and ■: Pt/S-CZ55.[77]

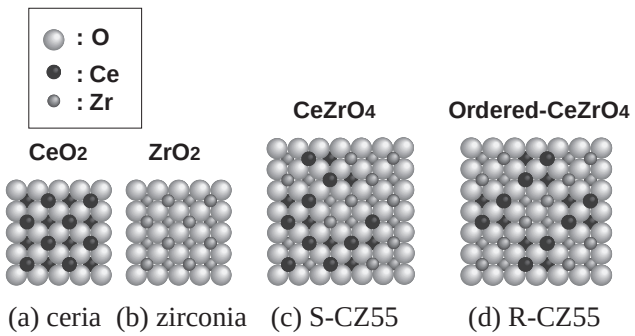

Fig. 9. Schematic illustration of atomic coordination: (a) cubic ceria, (b) cubic zirconia, (c) S-CZ55 and (d) R-CZ55 viewed perpendicular to the (100) plane.[78–80]

structure because the value of the calculated lattice is one half of the real lattice constant of the pyroclore structure. The dependence of the lattice constant on the zirconia content obeys Vegard's law in the series of S-CZs in Fig. 10. This shows that the milled powders consist of almost single phase ceria–zirconia solid solutions above a zirconia content of 50 mol% regardless of milling time, as estimated from XRD results as well as the solid solutions prepared by the homogeneous coprecipitation process. The bend in the curve at 50 mol% zirconia in the series of R-CZs in Fig. 11 confirms the identification of the structure in Table 2.

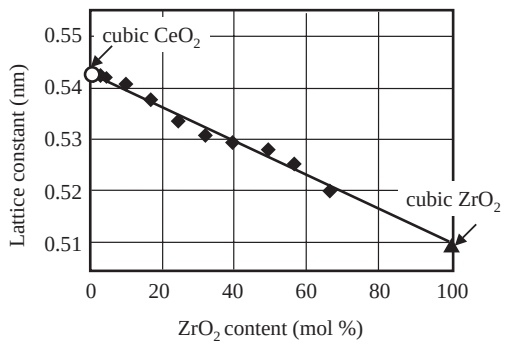

Fig. 10. Lattice constant calculated from the (311) peak of the fluorite structure as a function of ZrO_2 content in the formation of ceria–zirconia solid solution (S-CZ) during high-energy attrition milling of CeO_2 using a zirconia mill and zirconia balls in ethanol.[69]

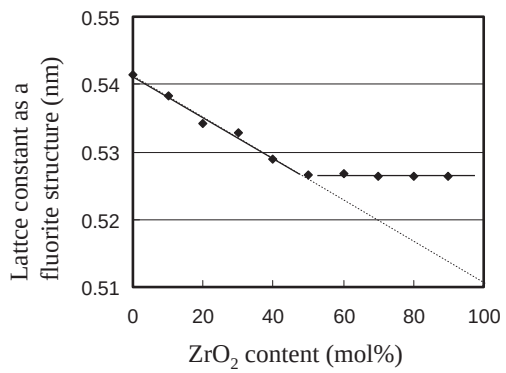

Fig. 11. Lattice constant calculated from the (311) peak of the fluorite structure as a function of ZrO_2 content in the ceria–zirconia solid solution (R-CZ). For the pyroclore structure, the (622) peak was regarded as the (311) peak of the fluorite structure assuming that the value of the calculated lattice constant is one half of the real lattice constant of the pyroclore structure.[75]

Since 1995, dissolution of ZrO_2 into the CeO_2 lattice has been reported over the entire composition range, yielding a cubic fluorite-type solid solution for ZnO_2 content not exceeding

50 mol% through the sol–gel process followed by heat-treatment at temperatures below 1000 °C.[55–63]

2.2 OSC of Second-Generation CZ and Catalytic Performance of Catalyst Containing Second-Generation CZ. The extent and rate of the oxidation–reduction process are dependent on the state of the dispersion of the ceria–zirconia mixed oxide, the presence and dispersion of precious metal components, and on the temperature and partial pressure of gaseous agents.[22] In general, oxygen storage/release capacity (OSC) is measured by temperature-programmed reduction (TPR) and total OSC is detected as pulse re-oxidation at a fixed temperature. Quantitative dynamic-OSC measurements are carried out on the sample by increasing the temperature in a stepwise manner, and during the isothermal steps, alternately pulsing H_2 or CO and O_2 over the sample.[22,57,84,85]

To quantify oxygen storage/release capacity (OSC) of ceria–zirconia mixed oxides, we define the total and partial OSC as follows:[80,83] (1) the total OSC (μmol-O_2/g-specimen) is defined as the weight loss/gain of a specimen, as measured by a thermogravimetric analyzer, upon exposure to a feed stream of hydrogen or oxygen in nitrogen at a fixed temperature until no more weight loss/gain occurs; and (2) the partial OSC (mol-O_2/mol-Ce) is calculated from the total OSC as the amount of oxygen released from one mole of CeO_2 in the specimen in a reducing atmosphere. Thus, the total OSC corresponds to OSCC (oxygen storage capacity complete) as defined by Yao et al.[21]

Figure 12 shows the total OSC value at 500 °C as a function of the zirconia content in mixed oxides (Ce/Zr = 9/1, 8/2, 75/25, 7/3, 6/4, 5/5, 4/6, 3/7, 25/75, 2/8, or 1/9) prepared by homogeneous coprecipitation followed by heat-treatment at 400 °C in air. In the figure, the OSC was not less than 250 μmol-O_2/g for Ce/Zr ratios between 75/25 and 25/75.[68] In particular, at a Ce/Zr ratio of 5/5, the OSC was at a maximum: about 450 μmol-O_2/g. This value corresponds to about 0.14 mol-O_2/mol-Ce of the partial OSC; it also means that about 55% of Ce^{4+} is converted into Ce^{3+} for cerium ions in the mixed oxide when the ratio of Ce/Zr is 5/5 because the partial OSC reaches the ideal value of 0.25 mol-O_2/mol-Ce when all Ce^{4+} ions transform into Ce^{3+}. Fornasiero et al.[55] and Balducci et al.[56] have obtained similar values (50–60% Ce^{3+}) for the O_2 uptake (corresponds to partial OSC) of a

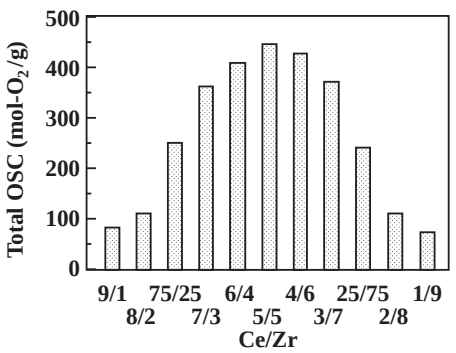

Fig. 12. The total OSC at 500 °C as a function of the ratio of cerium to zirconium (Ce/Zr) in mixed oxides prepared by homogeneous coprecipitation: The OSC of the oxides with 1.0 wt% Pt was measured.[68]

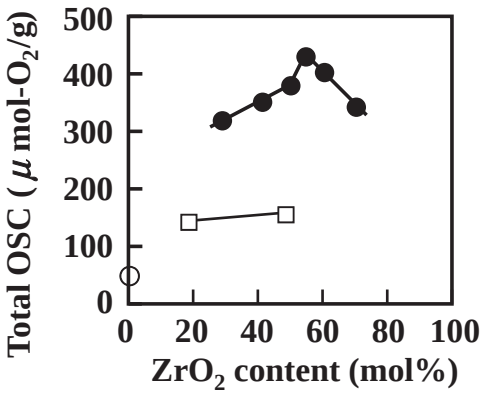

Fig. 13. The total OSC at 500 °C of the first- (□) and second-generation (■) CZ with 1 wt% Pt as a function of ZrO_2 content after heat-treatment at 700 °C, compared with that of CeO_2 (○) with 1 wt% Pt.[86]

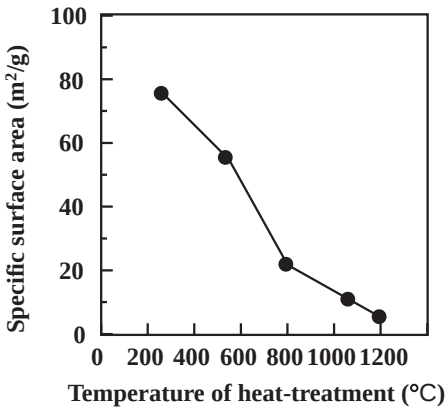

Fig. 14. The specific surface area of the ceria–zirconia solid solutions (Ce/Zr = 5/5) prepared by homogeneous coprecipitation using cerium(III) nitrate, zirconium(IV) bis(nitrate) oxide hydrate, ethylene oxide-propylene oxide block copolymer mono(2-ethylhexyl) ether and hydrogen peroxide as a function of heat-treatment temperature.[68]

$Ce_{0.5}Zr_{0.5}O_2$ solid solution prepared by a homogeneous gel route from [Ce(acac)$_4$] and Zr(OBu)$_4$ precursors.

Figure 13 shows the total OSC value at 500 °C as a function of the zirconia content in mixed oxides (Ce/Zr = 7/3, 6/4, 5/5, 45/55, or 3/7) after thermal aging at 700 °C in air.[86] The value of the maximum OSC in Fig. 13 was almost the same as that in Fig. 12; however, the value shifted to a zirconia content of 55 mol%. At the same time, the specific surface area decreased with increasing aging temperature. This is presumably because of the rearrangement of cerium and zirconium ions in the mixed oxide and the concomitant increase in the number of oxygen atoms surrounded by zirconium ions, which surpasses the number of oxygen atoms surrounded by cerium ions in the Ce/Zr < 1 range. This is because oxygen surrounded by zirconium ions is easier to store and release under lean and rich conditions, respectively, as assumed from the formation of pyroclore-type $Ce_2Zr_2O_7$,[87] which will be discussed later.

Figures 14 and 15 plot the specific surface area and average crystallite diameter, respectively, as a function of heat-treatment temperature for a ceria–zirconia solid solution

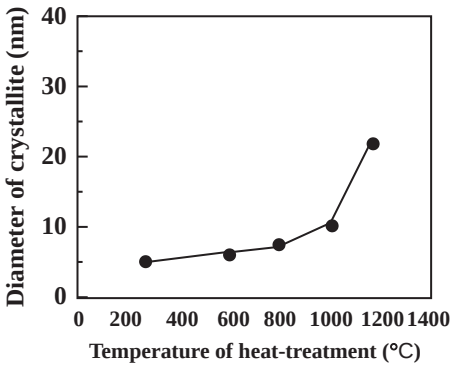

Fig. 15. The average crystallite diameter of ceria–zirconia solid solutions (Ce/Zr = 5/5), prepared by homogeneous coprecipitation using cerium(III) nitrate, zirconium(IV) bis(nitrate) oxide hydrate, ethylene oxide-propylene oxide block copolymer mono(2-ethylhexyl) ether and hydrogen peroxide as a function of heat-treatment temperature.[68]

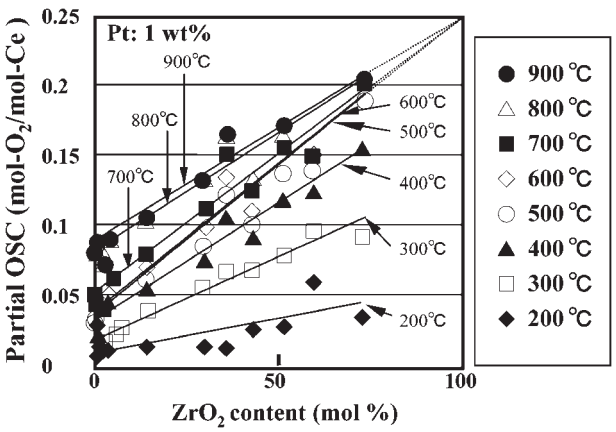

Fig. 16. Temperature dependence of partial OSC at a fixed temperature of ceria–zirconia solid solutions (S-CZ) milled in ethanol as a function of ZrO_2 content in the specimens. The OSC of the oxides with 1.0 wt % Pt was measured. Each line was drawn by the least square method.[83]

(Ce/Zr = 5/5) prepared by homogeneous coprecipitation using cerium(III) nitrate, zirconium(IV) bis(nitrate) oxide hydrate, ethylene oxide-propylene oxide block copolymer mono(2-ethylhexyl) ether as surfactant and hydrogen peroxide as oxidizing agent.[66] As can be seen in Figs. 14 and 15, even when the ceria–zirconia solid solution was heated in air at 1200 °C, the solid solution had a specific surface area of about 6 m^2/g, which is relatively large. Further, the average diameter could be maintained below 25 nm even though the specific surface area decreased with temperature.

The temperature dependence of the partial OSC of the ceria–zirconia solid solution prepared by the high-energy ball milling process is shown in Fig. 16.[83] The OSC in Fig. 16 is directly related to the nonstoichiometry of cerium oxide. Thus, the increase of OSC with temperature suggests the increased occurrence of nonstoichometry change in ceria with temperature. In ceria, nonstoichiometry is related to the occurrence of oxygen vacancies. Thus, OSC increases with the number of oxygen vacancies, which occur easily at higher temperatures in ceria. The extrapolation of the data for a given temperature yields 0.25 mol-O_2/mol-Ce for the 500–900 °C temperature range. This value can only be realized if every cerium(IV) transforms into cerium(III). This indicates that the cerium ion transforms completely into cerium(III) in extremely diluted solid solutions. Below 500 °C, the transformation to cerium(III) is incomplete. Only 30% of the cerium ion in pure ceria can be reduced to cerium(III), even at 900 °C. The OSC (Fig. 16) at temperature T for a solid solution ($Ce_{1-x}Zr_xO_2$) with x mol% ZrO_2, $Q(x,T)$, can be approximated by the following equation:

$$Q(x,T) \fallingdotseq \{(100-x)q(0,T) + xq(100,T)\}/100. \quad (4)$$

The variables $q(100,T)$ and $q(0,T)$ denote the OSC at T of pure cerium oxide and of an extremely diluted solid solution, respectively.

The dependence of OSC on ZrO_2 content in the solid solution suggests that the presence of Zr ions promotes the occurrence of cerium(III). The effective ionic radii of Ce^{4+}, Ce^{3+}, Zr^{4+}, and O^{2-} are 0.097, 0.114, 0.084, and 0.138 nm, with coordination numbers of 8, 8, 8, and 4, respectively, based on that of O^{2-} (0.140 nm) with a coordination number of 6.[41] Thus, the change of cerium(IV) into cerium(III) results in a volume increase, which would restrict further change due to the increased stress energy. The presence of the smaller Zr^{4+} ion could compensate for the volume increase. This is presumably the main reason why the presence of Zr ions promotes the valence change from IV to III, or III to IV in cerium ions, and the increase of OSC. The release of oxygen starts in a fully dense solid, a process which would be difficult, as shown in Table 3.[83] By contrast, in the storing process, oxygen has to migrate into the solid under the presence of oxygen vacancies, which is simpler than the release process. Thus, $t_r \gg t_s$, as shown in the table. Under the presence of Pt particles, HC, CO, and H_2 are rapidly oxidized, which means that either the reductive molecules or O^{2-} is activated by Pt. The escape of oxygen from the solid solution requires the transfer of electrons from oxygen to Ce^{4+} to Ce^{3+}, and a reaction with H and C. In the process, the reductive molecules play important roles in the release of oxygen in the atomic or ionic forms of H and C rather than in a molecular form. Pt activates these processes and shortens the reaction time. On the other hand, in the storing process, the migration of oxygen into the solid solution on-

Table 3. Time to Reach the Saturation of Storing and Releasing Oxygen and the Amount of Oxygen Stored or Released[83]

Time or amount	With Pt	Without Pt
Saturation time under oxidation condition in 50%O_2/N_2 : t_s	3 min	3 min
Saturation time under reduction condition in 50%H_2/N_2 : t_r	3 min	90 min
Amount of oxygen stored or released	384 μmol-O_2/ g-catalyst	384 μmol-O_2/ g-catalyst

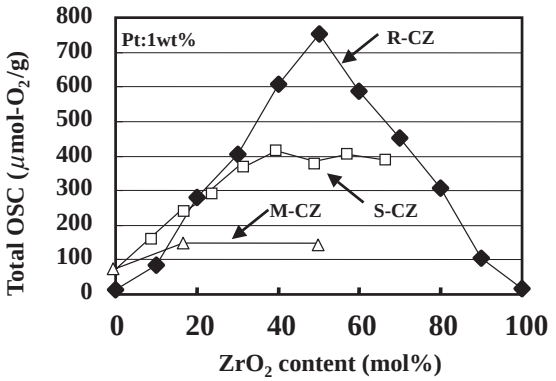

Fig. 17. Total OSC at 500 °C of ceria–zirconia mixed oxides reduced at 1200 °C in the presence of graphite followed by heating at 500 °C in air (R-CZ), milled in ethanol (S-CZ), and prepared by a solid–solid process followed by heat-treatment at 700 °C in air (M-CZ) with 1 wt% Pt as a function of ZrO_2 content in the specimens.[75,83]

ly needs the transfer of electrons from Ce^{3+} to oxygen, which is a much simpler process than the release process. The simplicity of the process, along with the presence of vacancies and smaller zirconium ions, explains why t_s is shorter than t_r.

Figure 17 plots total OSC vs zirconia content for ceria–zirconia mixed oxides (S-CZ) prepared by high-energy attrition milling or solid–solid reaction at 700 °C (M-CZ) with or without subsequent heating under reducing conditions at 1200 °C (R-CZ).[75,83] As seen in Fig. 17, the OSC of the sample prepared by the milling process increases with zirconia content in the lower-zirconia-content region, and remains constant in the relatively higher-zirconia-content region. The maximum OSC of the solid solution prepared by the milling process (S-CZ55) is three times larger than that obtained by solid–solid milling (M-CZ55). The maximum OSC of the reduced solid solution occurred at the composition of Ce/Zr = 5/5 (R-CZ55), and was about 753 μmol-O_2/g, which is about 1.8 times the maximum value (416 μmol-O_2/g) for the attrition milled solid solution and 5 times higher than that corresponding to the first-generation CZ (150 μmol-O_2/g). OSC is responsible for the difference in the solid solubility of zirconia in CZ. Considering only the high oxygen storage–release capacity, the reduced CZ (Ce/Zr = 5/5) should yield a pyroclore-type $Ce_2Zr_2O_7$ as a final structure because partial OSC reaches a maximum, or the ideal value of 0.25 mol-O_2/mol-Ce, when all of the Ce^{4+} in the reduced CZ changes into Ce^{3+}. As Ce and Zr in the solid solution often form the κ-phase $Ce_2Zr_2O_8$[81,82] or pyroclore-type $Ce_2Zr_2O_7$,[87,88] the OSC of the solid solution is higher. The number of surface oxygen atoms was estimated from the specific surface area of the attrition milled S-CZ55, reduced R-CZ55, and impregnated M-CZ55 mentioned in chapter 2.2.[77,89] That number should be about 3 μmol/m^2 for S-CZ55, R-CZ55, and M-CZ55. However, the experimental values were 530, 15.5, and 1.7 μmol/m^2 for Pt/R-CZ55, Pt/S-CZ55, and Pt/M-CZ55, respectively. Thus, the reduction of Pt/M-CZ55 is restricted at the surface. In Pt/S-CZ55, reduction proceeds up to about 5 layers into the surface. Of course, in Pt/R-CZ55, all bulk oxygen atoms participate in the redox process.

Table 4. Apparent Activation Energy of Oxygen Release from Pt/CeO_2–ZrO_2 Catalysts[77]

Catalyst	Apparent activation energy
Pt/M-CZ55	11 kJ mol^{-1}
Pt/S-CZ55	32 kJ mol^{-1}
Pt/R-CZ55	103 kJ mol^{-1}

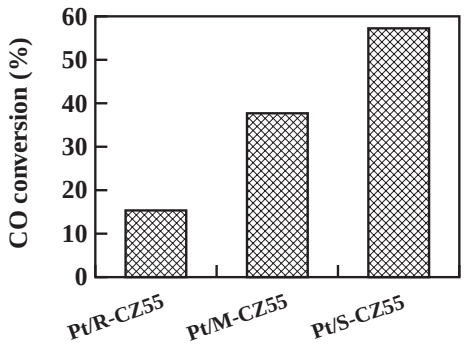

Fig. 18. CO conversion at 200 °C in the simulated exhaust reaction oscillating around the stoichiometric condition.[77]

Under real automotive catalyst operating conditions, the exhaust gas oscillates at a frequency of the order of 0.1 to 10 Hz. Thus, the first part of the total OSC is an important contributing factor in the catalytic reaction. Table 4 shows the apparent activation energy for oxygen release from Pt/S-CZ55, Pt/R-CZ55, and Pt/M-CZ55.[77] The apparent activation energy for Pt/R-CZ55 was about 100 kJ/mol. This value is close to the activation energy of oxygen hopping in stabilized ZrO_2.[90] In Pt/R-CZ55, which has a very low specific surface area, bulk oxygen contributes to OSC. Thus, the activation energy measured for Pt/R-CZ55 reflects the energy for oxygen hopping in the bulk of R-CZ55 oxide. The apparent activation energies of Pt/S-CZ55 and Pt/M-CZ55 are lower than that of Pt/R-CZ55. Reduction in these oxides is restricted to the surface or the sub-surface region. In such CZ oxides, the activation energy reflects the energy required for oxygen migration at the surface or subsurface. Figure 18 shows the conversion of CO at 200 °C under simulated automotive exhaust gas conditions over Pt/S-CZ55, Pt/R-CZ55, and Pt/M-CZ55 catalysts.[77] Pt/S-CZ55 showed the highest catalytic activity. The order in activity is well correlated with the order in the initial rate of oxygen release at 200 °C. This indicates that the initial rate of oxygen release (OSC) would be the best parameter to measure in order to get an insight on the catalytic activity under actual operating conditions.

Thus, we found that the ceria–zirconia solid solutions prepared by the homogeneous coprecipitation process and by the high energy attrition milling process both gave a maximum OSC at around 50 mol% zirconia. We have called these second-generation CZs. OSC of the catalyst containing second-generation CZ was about three times as high as that containing first-generation CZ and was superior to the latter in NOx emission reduction performance by about 40%.[76] As a result, in 1997 the modified three-way catalyst containing the second generation CZ was installed in vehicles in accordance with

the more stringent Low Emission Vehicle (LEV) exhaust regulation in California and in other places.

3. Development of the Third-Generation CZ (ACZ) and the Three-Way Catalyst Containing ACZ

In the latter half of the 1990s, even the three-way catalyst containing second-generation CZ for purifying exhaust gases would fail to satisfy the more severe exhaust regulations to be applied after 2000. Thus, it was necessary to develop a three-way catalyst with better heat resistance and greater oxygen storage capacity than that containing the second generation CZ.

Figures 19 and 20 plot the specific surface area, mean particle size and OSC of a 1-wt %-Pt-pellet-catalyst added ceria zirconia solid solution corresponding to a second-generation CZ (the CZ pellet catalyst) as a function of temperature during severe durability tests at high temperature for 3 h in air.[94,96] OSC of the sample was measured by calculating the amount of oxygen consumed from the amount of CO_2 generated at 500 °C by the alternate flow of 1% O_2 in nitrogen, followed by 2% CO in nitrogen. Specific surface areas were measured by the BET method. As shown in Figs. 19 and 20, the specific surface area and OSC of the CZ pellet catalyst decreased with temperature during the severe durability test, while the average size of the CZ particles in the pellet catalyst increased with temperature.

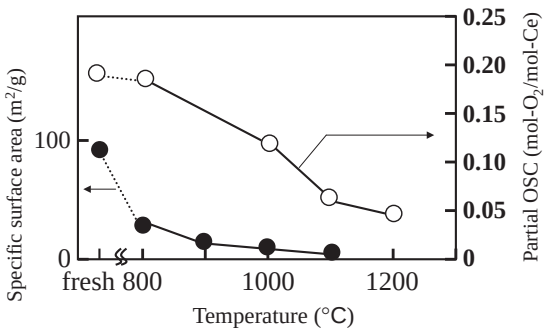

Fig. 19. The specific surface area and partial OSC of the CZ pellet catalyst with 1 wt % Pt as a function of temperature during severe durability test.[94,96]

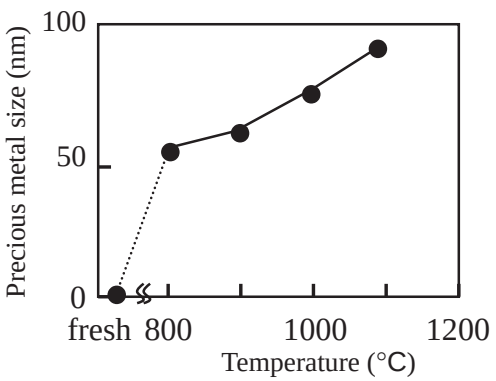

Fig. 20. Precious metal particle size of Pt on the CZ pellet catalyst with 1 wt % Pt as a function of temperature during severe durability test.[94]

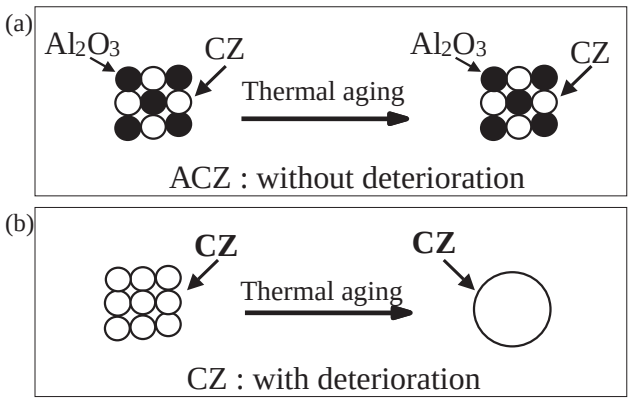

Fig. 21. New diffusion barrier concept: (a) ACZ, with alumina particles as dispersoids in CZ, inhibiting the grain growth of CZ and of the alumina itself; (b) and CZ, without any dispersoids, resulting in grain growth and decrease in activity.[80,94–96]

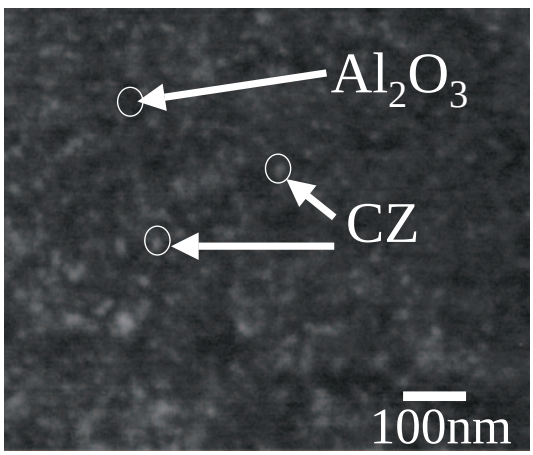

Fig. 22. SEM photograph of the cross section of ACZ powder after a 10-h durability test at 1000 °C in air.[95]

A new diffusion barrier concept was established to improve the heat resistance of the second-generation CZ, which is shown in Fig. 21.[80,94–96] In general, particles of a particular kind will easily coagulate or sinter at relatively low temperatures in air (Fig. 21b). However, if one particle type is isolated by another particle type, which does not react with neighboring particles at high temperature, the former particles do not coagulate or sinter (Fig. 21a). Based on this new diffusion barrier concept, we developed a catalyst containing third-generation CZ (ACZ),[91–93] consisting of nanometer-sized mixed oxides composed of alumina (A) and CZ having the same composition as second-generation CZ.

3.1 Preparation Process and Structure of Third-Generation CZ (ACZ). Third generation CZ (ACZ) was developed using the same homogeneous coprecipitation process as mentioned before and a sol–gel process, followed by heating of the precipitate. This concept is described in Fig. 22 and Table 5. Figure 22 shows an SEM micrograph of the cross section of ACZ particles prepared by homogeneous coprecipitation after being subjected to a thermal durability test for 10 h at 1000 °C.[95] In Fig. 22, the dark portions correspond to alumina;

Table 5. Particle Diameters of Pt and CZ after Lean–Rich Cycling Durability Test at Inlet Temperature of 900 °C (at Catalytic Temperature of about 950 °C)[94–96]

	ACZ-containing catalyst[a)]	CZ-containing catalyst[b)]
Pt particles	19.6 nm	23.7 nm
CZ particles	8.7 nm	17.2 nm

a) ACZ-containing catalyst contains the third-generation CZ (ACZ). b) The CZ-containing catalyst contains the second-generation CZ.

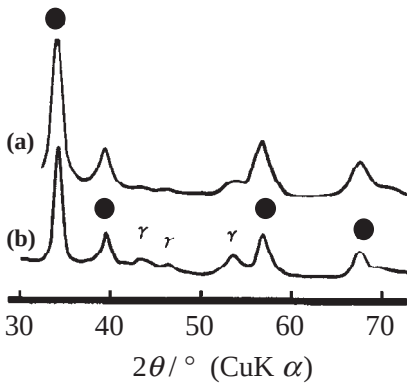

Fig. 23. XRD profiles of (a) ACZ-containing catalyst and (b) CZ-containing catalyst after a 5-h durability test in air at 1000 °C: ●: CZ; γ: γ-alumina.[94–96]

the bright portions correspond to CZ. The CZ particles in the ACZ are several nm in diameter and are dispersed in the alumina matrix as diffusion barriers. In addition, EDX analysis revealed that the X-ray intensity ratios of Ce/(Al + Ce + Zr) and Zr/(Al + Ce + Zr) were almost constant over several micrometer-sized regions in the SEM image. Thus, ACZ had a uniform constitutional distribution at the micrometer scale, even after a 10-h heat resistance test at 1000 °C. Figure 23 shows the XRD profiles of an ACZ-containing catalyst and a CZ-containing catalyst after a 5-h durability test at 1000 °C in air. These profiles indicated that the ceria components in both catalysts were in the presence of ceria–zirconia solid solutions. Table 5 shows the particle diameter of the precious metal (Pt) on the catalyst and the crystal size of the CZ in the catalyst after a lean/rich cyclic durability test at the inlet temperature of 900 °C.[94–96] As seen in Table 5, the sintering of Pt on the ACZ-containing catalyst is inhibited more effectively than that on the CZ-containing catalyst. Thus, the nanostructure of ACZ is regarded as an embodiment of the diffusion barrier concept. Figure 24 shows the specific surface area of ACZ and second-generation CZ as a function of temperature under a 10-h durability test in air. In Fig. 24, the specific surface area of the ACZ was, as expected, larger than that of the CZ after durability testing in air between 900 and 1200 °C. ACZ retains a larger specific surface area than CZ does even at the high temperature region around 1000 °C.[94–96]

3.2 OSC of ACZ and Catalytic Performance of a Catalyst Containing ACZ. Figure 25 shows the partial OSC of

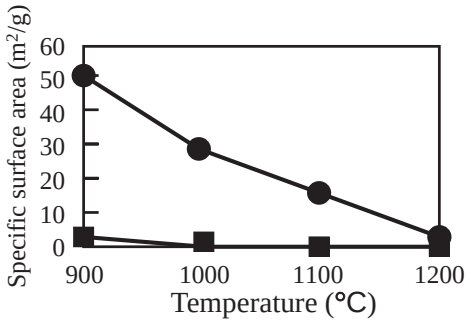

Fig. 24. Specific surface area of ACZ (●) and CZ (■) after a 10-h durability test in air.[94–96]

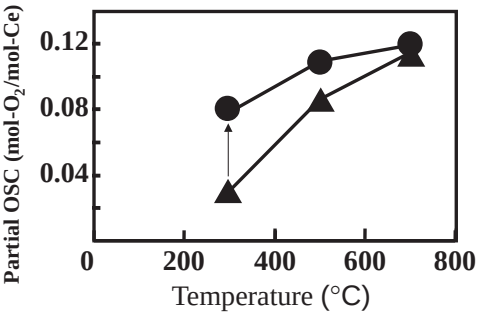

Fig. 25. The partial OSC of the Pt/ACZ catalyst (●) and Pt/(Al_2O_3 + CZ) catalyst (▲) after a 5-h thermal durability test at 1000 °C in air.[95]

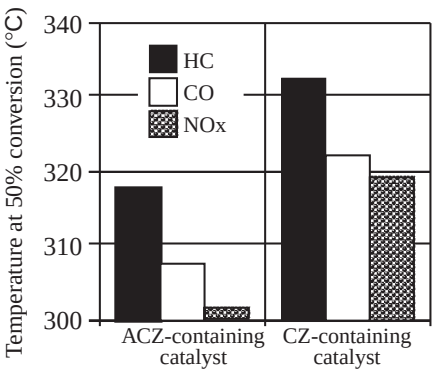

Fig. 26. Temperature at 50% conversion of HC (■), CO (□), and NOx (▩) on the ACZ-containing catalyst and CZ-containing catalyst after a 100-h durability test.[96]

Pt/ACZ and Pt/(Al_2O_3 + CZ) catalysts as a function of temperature after a 5-h thermal durability test at 1000 °C in air. The OSC of ACZ is higher than that of CZ throughout the temperature range.[95] The addition of ACZ improved OSC, especially at low temperature (≤300 °C). The high OSC activity of the Pt/ACZ catalyst at lower temperatures is responsible for the smaller particle size of the CZ in ACZ as compared to the CZ in the CZ–Al_2O_3 mixture (Table 5). Figure 26 shows the catalytic performance for HC, CO, and NOx emissions of ACZ- and the CZ-containing catalysts after a 100-h durability test, evaluated by installing these catalysts in vehicles with 2.2-liter engines.[96] The temperature at 50% conversion for HC, CO, and NOx on the ACZ-containing catalyst is about

15 °C lower than that on the CZ-catalyst.

Thus, ACZ can be used, not only as an oxygen storage material, but also as a support for precious metal particles. Even when exposed to exhaust gases at high temperature, the alumina in ACZ plays an important role as a diffusion barrier, and grain growth of CZ is suppressed. Besides, the specific surface area of ACZ is larger than that of second-generation CZ. The partial OSC of the catalyst involving third-generation CZ was about 2.5 times higher than that containing second-generation CZ. The catalyst containing third-generation CZ is superior to that containing second-generation CZ in NOx emission reduction performance by about 20%.[94–96] Thus, in 2001, the modified three-way catalyst containing ACZ was installed in vehicles in accordance with the more stringent Low Emission Vehicle II(LEVII) exhaust regulation in California, the year 2000-regulation in Japan. In 2002, vehicles were equipped with the modified catalyst containing ACZ in accordance with the most stringent Partial Zero Emission Vehicle (PZEV) exhaust regulation in California.[97]

4. Manufacturing Technique for Three-Way Catalysts Containing ACZ

Figure 27 shows the improvement in partial OSC for first- to third-generation CZ, compared to that of pure ceria in the presence of Pt. As shown in Fig. 27, the OSC of a three-way catalyst containing ACZ is about 23 times higher than that containing ceria.[80] Figure 28 shows the improvement in NOx emission

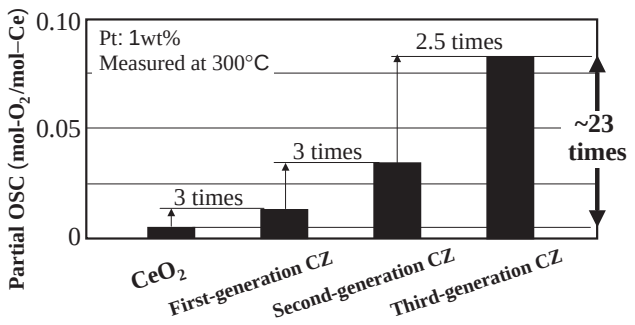

Fig. 27. Progress of the partial OSC of the developed ceria–zirconia solid solution after a 5-h durability test at 1000 °C in air.[80]

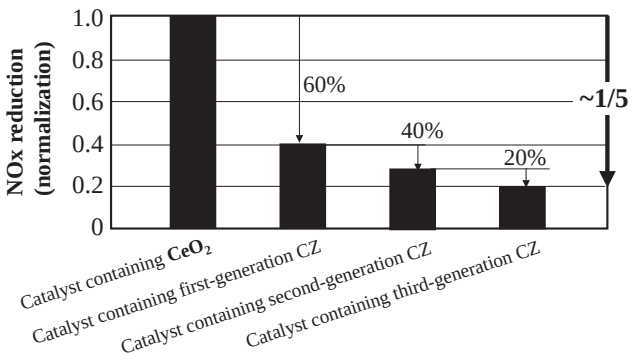

Fig. 28. Improvement in NOx emission reduction performance in the LA#4 driving cycle test for three-way catalysts containing a ceria–zirconia solid solution.

for three-way catalysts containing first- to third-generation CZ, compared to that containing pure ceria. The precious metal catalyst containing oxygen storage materials could significantly reduce the NOx emission. These oxygen storage materials have greatly contributed to catalytic systems for automotive exhaust gases. NOx emission over a catalyst containing ACZ is reduced to about 20% of that containing ceria. Thus, the loading amount of precious metal over the catalyst containing ACZ was reduced to about 1/2 that containing pure ceria.

The above-mentioned catalysts containing first- to third-generation CZ are manufactured by wash-coating a slurry composed of precious metal particles, CZ, and alumina on the surface of a honeycomb substrate wall, however, this manufacturing technique is complicated. The technique for each generation CZ was conformed for the first time to succeed in the control of the CZ particle size and surface features of the catalyst.

The Toyota Motor Corp. has put automotive three-way catalysts containing first-, second-, and third-generation CZs into practical use globally in 1989, 1997, and 2001, respectively.

X-ray diffraction analysis and electron diffraction analysis have recently revealed that a pyroclore phase $Ce_2Zr_2O_7$ (space group: $Fd\bar{3}m$) left in air for about one year is transformed to a meta-stable $Ce_2Zr_2O_{7.5}$ (space group: $F\bar{4}3m$).[98] This indicates that the Zr^{4+} ion is much more likely to combine with 7 oxide ions and hence exhibit a coordination number of 7, rather than 6 or 8, in the presence of cerium ions in the lattice of the ceria–zirconia solid solution in air at room temperature. This property of the Zr^{4+} ion, i.e., its strong tendency to exhibit a coordination number of 7 is thought to be the driving force behind the oxygen storage/release capacity. EXAFS, Raman spectroscopy,[99] and pulse neutron diffraction analysis[100] reveal that there is somewhat of a difference in the local arrangement of oxide ions between the two kinds of solid solutions identified as having the same structure by XRD. Furthermore, studies have been reported on oxygen migration processes in ceria–zirconia solid solutions and on dynamic changing from Ce^{3+} to Ce^{4+} or Ce^{4+} to Ce^{3+} using, respectively, Isotope Exchange reactions[101,102] and in situ Time-Resolved Energy-Dispersive XAFS.[103]

Studies on lattice metal and lattice oxygen will soon yield a new mechanism for high oxygen storage and release capacity.

We lead the research and development through patents, lectures in domestic and international conferences, general and interpretive articles, and publications. These series of technologies have become a de facto standard in the field of three-way catalysts in the world.

The authors wish to thank Dr. Kamigaito, the former president of Toyota Central R&D Labs., Inc. for his helpful advice throughout the work. The authors also wish to thank Professor Dupretz and Dr. Descorme of Poitier University for their collaborative advice and Professor Kašpar and co-workers of Trieste University for their valuable discussions. The authors are also grateful to their co-workers for their continued support and would like to acknowledge that the development of automotive exhaust catalysts containing first- through third-generation CZ was the result of a joint effort by the Toyota Motor Corp. and the Toyota Central R&D Labs., Inc. in Japan.

References

1 G. J. Barnes, R. L. Klimisch, and B. B. Krieger, *SAE Paper* 730200 (1973).

2 Y. Kaneko, H. Kobayashi, O. Hirako, and O. Nakayama, *SAE Paper* 780607 (1978).

3 J. H. Jones, J. T. Kummer, K. Otto, M. Shelef, and E. E. Weaver, *Environ. Sci. Technol.*, **5**, 790 (1971).

4 G. J. K. Acres and B. J. Cooper, *JP Laid-Open* No. 48-63985, Filed 22/11/1972.

5 J. G. Rivard, *SAE Paper* 730005 (1973).

6 I. Gorille, N. Rittmansberger, and P. Werner, *SAE Paper* 750368 (1975); R. Zechnall, G. Baumann, and H. Eisele, *SAE Paper* 730566 (1973).

7 JP 999752, Filed 04/06/1974; T. Omori and K. Oiwa, *JP Laid-Open* No. 49-57226, Filed 04/06/1974.

8 JP No. 1123788, Filed 19/10/1972; K. Endo, J. Kawaharada, M. Sueishi, and H. Norimatsu, *JP Laid-Open* No. 49-63830, Filed 19/10/1972.

9 JP No. 967909, Filed 23/10/1972; O. Ogawa, T. Omori, and S. Harada, *JP Laid-Open* No. 49-64721, Filed 23/10/1972.

10 H. Dueker, K.-H. Friese, and W.-D. Haecker, *SAE Paper* 750223 (1975); K.-H. Friese, H. Gaiel, R. Bornel, and H. Schalert, JP No. 943275, Filed 09/03/1973; K.-H. Friese, H. Gaiel, R. Bornel, and H. Schalert, *JP Laid-Open* No. 49-1285, Filed 09/03/1973.

11 USP. No. 3815561 Filed 14/09/1972; W. R. Seits, *JP Laid-Open* No. 49-68122 Filed 12/09/1973.

12 JP No. 928463, Filed 31/07/1973; T. J. Himac, *JP Laid-Open* No. 49-60785, Filed 31/07/1973.

13 H. S. Gandhi, A. G. Piken, M. Shelef, and R. G. Delesh, *SAE Paper* 760201 (1976); H. S. Gandhi, A. G. Piken, H. K. Stepien, M. Shelef, R. G. Delesh, and M. E. Heyde, *SAE Paper* 770196 (1977).

14 J. C. Schlatter, *SAE Paper* 780199 (1987).

15 J. T. Kummer, "Proceedings of Energy Combustion Science," Vol. 6, Pergamon, Great Britain (1980), p177, and references therein.

16 JP No. 865370, Filed 03/10/1972; O. Kamigaito, H. Doi, K. Sano, T. Kandori, Y. Oyama, and H. Masaki, *JP Laid-Open* No. 49-55584, Filed 03/10/1972.

17 JP No. 935113, Filed 14/02/1973; N. Komatsu, O. Kamigaito, T. Suzuki, H. Doi, K. Sano, O. Yamamoto, T. Kandori, and M. Tsuzuki, *JP Laid-Open* No. 49-106487, Filed 14/02/1973.

18 JP No. 958489, Filed 03/04/1973; N. Komatsu, O. Kamigaito, T. Suzuki, O. Yamamoto, H. Doi, K. Sano, T. Kandori, and M. Tsuzuki, *JP Laid-Open* No. 49-123473, Filed 03/04/1973.

19 JP No. 1033368, Filed 14/11/1972; N. Komatsu, O. Kamigaito, T. Suzuki, H. Doi, K. Sano, O. Yamamoto, T. Kandori, and M. Tsuzuki, *JP Laid-Open* No. 49-71313, Filed 14/11/1972.

20 R. K. Herz, *Ind. Eng. Chem. Prod. Rev.*, **20**, 451 (1981).

21 H. C. Yao and Y. F. Yu Yao, *J. Catal.*, **86**, 254 (1984).

22 E. C. Su, C. N. Montreuil, and W. G. Rothschild, *Appl. Catal.*, **17**, 75 (1985).

23 JP No. 1290398, Filed 13/03/1975; M. Taguchi, K. Funabiki, S. Kawagoe, and M. Kubo, *JP Laid-Open* No. 51-104491, Filed 13/03/1975.

24 JP No. 1330556, Filed 16/04/1982; M. Sato and T. Kawai, *JP Laid-Open* No. 57-63133, Filed 16/04/1982.

25 N. Miyoshi, S. Matsumoto, M. Ozawa, and M. Kimura, *SAE Paper* 891970 (1989).

26 N. Miki, T. Ogawa, M. Haneda, N. Kakuta, A. Ueno, S. Tateishi, S. Matsuura, and M. Sato, *J. Phys. Chem.*, **94**, 6464 (1990).

27 S. Matsumoto, N. Miyoshi, T. Kanazawa, M. Kimura, and M. Ozawa, "Catal.: Sci. Technol.," ed by S. Yoshida, T. N. Tabezawa, and T. Ono, Kodansha-VCH (1991), Vol. 1, p. 335.

28 Y. Watanabe, A. Banno, and M. Sugiura, *Appl. Clay Sci.*, **16**, 59 (2000).

29 K. Yamazaki, N. Takahashi, H. Shinjoh, and M. Sugiura, *Adv. Tech. Mat. & Mat. Proc. J.*, **4**, 1 (2002).

30 B. J. Cooper and L. Keck, *SAE Paper* 800461 (1980).

31 E. C. Su, C. N. Montreuil, and W. G. Rothschild, *Appl. Catal.*, **17**, 75 (1985).

32 M. Ohashi, *Syokubai (Catalyst)*, **29**, 598 (1987).

33 USP 4927799, Filed 27/12/1988; DEP 3737419, Filed 04/11/1987; JP 2140560 Filed 04/11/1986; JP 1881751, Filed 04/11/1986; S. Matsumoto, N. Miyoshi, M. Kimura, M. Ozawa, and A. Isogai, *JP Laid-Open* No. 63-116741, Filed 04/11/1986; S. Matsumoto, N. Miyoshi, M. Kimura, M. Ozawa, and A. Isogai, *JP Laid-Open* No. 63-116742, Filed 04/11/1986.

34 USP 5075276, Filed 30/04/1988; JP 1922065, Filed 30/04/1988; M. Ozawa, M. Kimura, A. Isogai, S. Matsumoto, and N. Miyoshi, *JP Laid-Open* No. 1-281144, Filed 30/04/1988.

35 EP 337809, Filed 14/04/1989; S. Kitaguchi, K. Tsuchitani, and T. Ohata, *JP Laid-Open* No. 2-43951, Filed 14/04/1989.

36 JP 2858945, Filed 08/06/1990; M. Funabiki, K. Kanihide, and T. Yamada, WO 90-14888, Filed 08/06/1990.

37 T. Kamo, Y. Chujo, T. Akatsuka, J. Nakano, and M. Suzuki, *SAE paper* 850380 (1985).

38 K. Saji, H. Kondo, T. Takahashi, and I. Igarashi, *J. Electrochem. Soc.*, **135**, 1686 (1988).

39 J. F. Baumard and P. Abelard, *Adv. Ceram.*, **12**, 555 (1984).

40 M. Ozawa, M. Kimura, and A. Isogai, *J. Alloys Compd.*, **193**, 73 (1993).

41 R. D. Shannon and C. T. Prewitt, *Acta Crystallogr., Sect. B*, **25**, 925 (1969).

42 P. Duwez and F. Odell, *J. Am. Ceram. Soc.*, **33**, 274 (1950).

43 E. Tani, M. Yoshimura, and S. Somiya, *J. Am. Ceram. Soc.*, **66**, 506 (1983).

44 F. Duran, M. Gonzalez, C. Moure, and C. Pasucual, *J. Mater. Sci.*, **25**, 5001 (1990).

45 M. Ozawa, *J. Alloys Compd.*, **275/277**, 886 (1998).

46 M. Kimura, M. Ozawa, and S. Matsumoto, "Proceeding of the Thirds Workshop on Functional Nonstoichiometric Oxides," Catalysis Society of Japan (1990).

47 J. Kašpar, P. Fornasiero, and M. Graziani, *Catal. Today*, **50**, 285 (1999).

48 C. de Leitenburg, A. Trovarelli, F. Zamar, S. Maschio, G. Dolcetti, and J. Llorca, *J. Chem. Soc., Chem. Commun.*, **1995**, 2181.

49 A. Trovarelli, F. Zamar, J. Llorca, C. de Leitenburg, G. Dolcetti, and J. T. Kiss, *J. Catal.*, **169**, 490 (1997).

50 T. Murota, T. Hasegawa, S. Aozasa, H. Matsui, and M. Motoyama, *J. Alloys Compd.*, **193**, 298 (1993).

51 C. de Leitenburg, A. Trovarelli, J. Llorca, F. Cavani, and G. Bini, *Appl. Catal., A*, **39**, 161 (1996).

52 A. Kawabata, S. Hirano, M. Yoshinaga, K. Hirota, and O. Yamaguchi, *J. Mater. Sci.*, **31**, 5945 (1996).

53 C. E. Hori, H. Permana, K. Y. S. Ng, A. Brenner, K. More,

K. M. Rahmoeller, and D. Belton, *Appl. Catal., B*, **16**, 105 (1998).
54 D. Terribile, A. Trovarelli, J. Llorca, C. de Leitenburg, and G. Dolcetti, *Catal. Today*, **43**, 79 (1998).
55 P. Fornasiero, J. Kašpar, and M. Graziani, *J. Catal.*, **167**, 576 (1997).
56 G. Balducci, P. Fornasiero, R. Di Monte, J. Kašpar, S. Meriani, and M. Graziani, *Catal. Lett.*, **33**, 193 (1995).
57 P. Fornasiero, G. Balducci, R. Di Monte, J. Kašpar, V. Sergo, G. Gubitosa, A. Ferrero, and M. Graziani, *J. Catal.*, **164**, 173 (1996).
58 S. Rossignol, T. Madier, and D. Duprez, *Catal. Today*, **50**, 261 (1999).
59 P. Vidmar, P. Fornasiero, J. Kašpar, G. Gubitosa, and M. Graziani, *J. Catal.*, **171**, 160 (1997).
60 M.-F. Luo, Y.-J. Zhong, X.-X. Yuan, and X.-M. Zheng, *Appl. Catal., A*, **162**, 121 (1997).
61 M.-F. Luo, G.-L Lu, X.-M Zheng, Y.-J. Zhong, and T.-H. Wu, *J. Mater. Sci. Lett.*, **17**, 1553 (1998).
62 C. K. Narula, L. P. Haack, W. Chun, H.-W. Chun, and G. W. Graham, *J. Phys. Chem., B*, **103**, 3634 (1999).
63 S. Rossignol, C. Descorme, C. Kappenstein, and D. Duprez, *J. Mater. Chem.*, **11**, 2587 (2001).
64 M. Yashima, K. Morimoto, N. Ishizawa, and M. Yoshimura, *J. Am. Ceram. Soc.*, **76**, 1745 (1993).
65 M. Yashima, K. Morimoto, N. Ishizawa, and M. Yoshimura, *J. Am. Ceram. Soc.*, **76**, 2865 (1993).
66 M. Yashima, H. Arashi, M. Kakihana, and M. Yashima, *J. Am. Ceram. Soc.*, **77**, 1067 (1994).
67 P. Fornasiero, R. Di Monte, G. R. Rao, J. Kašpar, S. Meriani, A. Trovarelli, and M. Graziani, *J. Catal.*, **151**, 168 (1995).
68 EP 0778071A1, Filed 06/12/1996; USP 5958827, Filed 04/12/1996; JP 3238316, Filed 07/12/1995; A. Suda, H. Sobukawa, T. Suzuki, T. Kandori, Y. Ukyo, M. Sugiura, M. Kimura, H. Hirabayashi, and Y. Ikeda, *JP Laid-Open* No. 9-155192, Filed 07/12/1995: JP 3341973, Filed 26/11/1996; A. Suda, H. Sobukawa, T. Suzuki, T. Kandori, Y. Ukyou, M. Sugiura, and M. Mareo, *JP Laid-Open* No. 9-221304, Filed 26/11/1996.
69 A. Suda, T. Kandori, N. Terao, Y. Ukyou, H. Sobukawa, and M. Sugiura, *J. Mater. Sci. Lett.*, **17**, 89 (1998).
70 A. Suda, T. Kandori, Y. Ukyou, H. Sobukawa, and M. Sugiura, *J. Ceram. Soc. Jpn.*, **108**, 473 (2000).
71 A. Suda, H. Sobukawa, T. Kandori, Y. Ukyou, and M. Sugiura, *J. Ceram. Soc. Jpn.*, **109**, 570 (2001).
72 G. Charlot, "L'analyse Qualitative et Les Reactions en Solution,", 4th ed., Masson, Paris (1957), Chap. 11, p. 81, and references therein.
73 No. 34-0394 for CeO_2, No. 27-0997 for ZrO_2 in JCPDS (Joint Committee on Powder Diffraction Standards) Cards.
74 C. S. Barrett, T. B. Massalski, "Structure of Metals," 3rd ed, McGraw-Hill, New York (1966), Chap. 13, p. 338, and references therein.
75 A. Suda, Y. Ukyou, H. Sobukawa, and M. Sugiura, *J. Ceram. Soc. Jpn.*, **110**, 126 (2002).
76 M. Sugiura, *Syokubai (Catalysts & Catalysis)*, **45**, 301 (2003).
77 T. Tanabe, A. Suda, C. Descorme, D. Duprez, H. Shinjoh, and M. Sugiura, *Stud. Surf. Sci. Catal.*, **138**, 135 (2001).
78 Y. Nagai, T. Yamamoto, T. Tanaka, S. Yoshida, T. Nonaka, T. Okamoto, A. Suda, and M. Sugiura, *J. Synchrotron Radiat.*, **8**, 616 (2001).
79 Y. Nagai, T. Yamamoto, T. Tanaka, S. Yoshida, T. Nonaka, T. Okamoto, A. Suda, and M. Sugiura, *Catal. Today*, **74**, 225 (2002).
80 M. Sugiura, *Catal. Surv. Asia*, **7**, 77 (2003).
81 T. Omata, H. Kishimoto, S. Otsuka-Yao-Matsuo, N. Ohtori, and N. Umesaki, *J. Solid State Chem.*, **147**, 573 (1999).
82 H. Kishimoto, T. Omata, S. Otsuka-Yao-Matsuo, K. Ueda, H. Hosono, and H. Kawazoe, *J. Alloys. Compd.*, **312**, 94 (2000).
83 A. Suda, H. Sobukawa, T. Suzuki, T. Kandori, Y. Ukyou, and M. Sugiura, *J. Ceram. Soc. Jpn.*, **109**, 177 (2001).
84 P. Fornasiero, J. Kašpar, and M. Graziani, *Appl. Catal., B*, **22**, L11 (1999).
85 J. Kašpar, R. Di Monte, P. Fornasiero, M. Graziani, H. Bradshaw, and C. Norman, *Top. Catal.*, **16/17**, 83 (2001).
86 H. Sobukawa, A. Suda, Y. Ukyo, T. Suzuki, M. Kimra, M. Sugiura, Y. Ikeda, and H. Hirayama, *Shokubai (Catalysts & Catalysis)*, **43**, 107 (2001).
87 R. Roth, *J. Res. Natl. Bur. Stand. (U.S.)*, **56**, 17 (1956).
88 S. Otsuka-Yao, H. Morikawa, N. Izu, and K. Okuda, *J. Jpn. Inst. Met.*, **59**, 1237 (1995).
89 Y. Madier, C. Descorme, A. M. Le Govic, and D. Duprez, *J. Phys. Chem.*, **103**, 10999 (1999).
90 J. F. Baumard and P. Abelard, *Adv. Ceram.*, **12**, 555 (1984).
91 JP 3330296, Filed 27/01/1997; T. Suzuki, H. Sobukawa, A. Suda, A. Morikawa, T. Kandori, M. Kimura, and M. Sugiura, *JP Laid-Open* No. 10-202101, Filed 27/01/1997.
92 EP 0834348A2, Filed 06/10/1997; USP 6150288, Filed 07/10/1997; USP 6306794B1, Filed 27/06/2000; JP 3262044, Filed 30/09/1997; T. Suzuki and H. Subukawa, *JP Laid-Open* No. 10-182155, Filed 30/09/1997.
93 EP 1020216B1, Filed 04/01/2000; USP 6335305B1, Filed 11/04/2000; JP 3265534, Filed 18/01/1999; T. Suzuki, A. Morikawa, and H. Sobukawa, *JP Laid-Open* No. 2000-271480, Filed 18/01/1999.
94 T. Kanazawa, J. Suzuki, T. Takada, T. Suzuki, A. Morikawa, A. Suda, H. Sobukawa, and M. Sugiura, 2002 JSAE Annual Congress, No. 52-2, 20025084, July 23–25, 2002, Yokohama, Japan, p. 9.
95 T. Kanazawa, J. Suzuki, T. Takada, T. Suzuki, A. Morikawa, A. Suda, H. Sobukawa, and M. Sugiura, *Stud. Surf. Sci. Catal.*, **145**, 415 (2002).
96 T. Kanazawa, J. Suzuki, T. Takada, T. Suzuki, A. Morikawa, A. Suda, H. Sobukawa, and M. Sugiura, *SAE Paper* 2003-01-0811 (2003).
97 T. Kidokoro, K. Hoshi, K. Hiraku, K. Satoya, T. Watanabe, T. Fujiwara, and H. Suzuki, *SAE Paper* 2003-01-0817 (2003).
98 T. Sasaki, Y. Ukyo, A. Suda, M. Sugiura, K. Kuroda, and H. Saka, *J. Ceram. Soc. Jpn.*, **111**, 382 (2003).
99 G. Vlanic, R. Di Monte, P. Fornasiero, E. Fonda, J. Kašpar, and M. Graziani, *Stud. Surf. Sci. Catal.*, **116**, 185 (1998).
100 E. Mamontov, T. Egami, R. Brezny, and M. Koranne, S. Tyagi, *J. Phys. Chem., B*, **104**, 11110 (2000).
101 F. Dong, A. Suda, T. Tanabe, Y. Nagai, H. Sobukawa, H. Shinjoh, C. Descorme, D. Duprez, and M. Sugiura, *Catal. Today*, **90**, 223 (2004).
102 F. Dong, A. Suda, T. Tanabe, Y. Nagai, H. Sobukawa, H. Shinjoh, C. Descorme, D. Duprez, and M. Sugiura, *Catal. Today*, **93/95**, 827 (2004).
103 A. Yamaguchi, T. Shido, Y. Inada, T. Kogure, K. Asakura, M. Nomura, and Y. Iwasawa, *Bull. Chem. Soc. Jpn.*, **74**, 801 (2001).

Masahiro Sugiura was born in 1942 at Aichi, Japan. After graduating from Nagoya University, he joined New Japan Chemical Co., Ltd. in 1967–1968, where he was engaged in development on alkylcyclohexanol and its derivative. After he received his master's degree at Nagoya University in 1971, he joined Toyota Central R&D Labs., Inc. He was engaged in studies on odorous analysis and odor control in 1972–1986 and on ultrafine oxides and ceramic materials in 1983–1986, in development of adsorptive and porous materials in 1986–1994, and finally in R&D on automotive catalysts from 1990 to this day. In 1994, he received his degree of Dr. Eng. at Nagoya University under the direction of Prof. Shin Tsuge, titled "Adsorption and Removal of Odorous Vapors by Sepiolite, Active Carbon and Complexes using them". He worked as an editorial board member for the Journal (Catalysts & Catalysis) of the Catalytic Society of Japan in 1998–2000. He received a 30th Machine Promotion Society Award, for his article titled "Lean-burn Engine Equipped with NOx Storage Reduction Type Three-Way Catalyst" in 1995, and an Award of the Outstanding Papers Published in the Journal of The Ceramic Society of Japan in 2004, for his article titled "Oxygen Absorption Behavior of $Ce_2Zr_2O_{7+x}$ and Formation of $Ce_2Zr_2O_{7.5}$". He retired from Toyota Central R&D Labs., Inc. in 2005. Now he works at Japan Synchrotron Radiation Research Institute (JASRI).

Masakuni Ozawa was born in 1957, at Aichi, Japan; he graduated from Nagoya University, M.A. in Chemistry, Doctor of Engineering from Nagoya University with a thesis, "Processing and characterization of ceramics modified with rare earth elements" under the direction of Prof. Shin-ichi Hirano. He worked in Toyota Central Res. Develop. Labs in 1981–1992, and joined Nagoya Institute of Technology (NIT) as an associate professor in 1993, then Professor of materials engineering at the graduate school of engineering, ceramics res. lab in NIT since 2004. His major study is inorganic and solid state chemistry, including ceramics and catalyst, for environmental pollution control. He worked as an editorial board member for the Journal of the Ceramic Society of Japan in 1999–2002, as a guest editor of the Journal of Alloys & Compounds in 2004, and received the Academic (Shiokawa) Award of the Rare Earth Society of Japan (2004).

Akihiko Suda was born in 1958, at Toyama, Japan. After graduating from Tohoku University in 1981, he entered the Graduate School of this University. He got his M.S. degree from Tohoku University in 1983. He joined Toyota Central R&D Labs., Inc. straight out of the Graduate School. He was engaged on an applied research of sepiolite from 1984 to 1989, and on a development of Si_3N_4, Sialon ceramics and ECR plasma etching technique of them, and on a development and application of ultrafine powder processing to mullite ceramics and automotive catalyst materials from 1989 to 1994, and on R&D of inorganic materials for automotive catalyst from 1995 to now. He received Technical Award of the Ceramic Society of Japan, for his paper titled "Development and practical application of ceria–zirconia solid solutions for automotive 3way catalysts" in 2003. He also received an Award of the Outstanding Papers Published in the Journal of The Ceramic Society of Japan in 2004, for his paper titled "Oxygen Absorption Behavior of $Ce_2Zr_2O_{7+x}$ and Formation of $Ce_2Zr_2O_{7.5}$". Now, he is a Project Manager of Applied Catalysis Lab. of Toyota Central R&D Labs., Inc.

Tadashi Suzuki was born in Aichi, Japan, in 1961. He graduated from the Department of Electrical Engineering, Faculty of Science & Technology, Meijo University in 1984. He has been working in Applied Catalysis Lab., Materials Dept. Toyota Central R&D Labs., Inc. He has been active in the field of micro and surface analyses and research and development of automotive catalysts. His main research is about three-way catalysts.

Takaaki Kanazawa was born in 1961 at Aichi, Japan. In 1983, when he graduated from the Department of Applied Physics, Basic Engineering, Tsukuba University, he joined Metal Material Dept., Toyota Motor Corporation. In 1990, he moved his assignment to Catalyst Design Dept., Toyota Motor Corporation. In 1993–1994, he was transferred to the Manager of Next Generation Catalyst Research Institute, Co., Ltd. In 1995, he returned to Toyota Motor Corporation. Since then, he has been active in the field of automotive catalysts as a Project Manager of Catalyst Design Dept, Material Engineering Div.1. His main research is about 3-way Catalysts, NOx Catalysts, and HC adsorbents.